A High-Yield Reproducible Synthesis of MCM-48 Starting from Fumed Silica

O. Collart,*,† P. Van Der Voort,† E. F. Vansant,† D. Desplantier,‡ A. Galarneau,‡ F. Di Renzo,‡ and F. Fajula‡

Laboratory of Adsorption and Catalysis, University of Antwerp (U.I.A.), Universiteitsplein 1, 2610 Wilrijk, Belgium, and Laboratoire de Matériaux Catalytiques et Catalyse en Chimie Organique, Ecole Nationale Supérieure de Chimie de Montpellier, 8 rue de l'Ecole Normale, 34296 Montpellier Cedex 5, France

Received: August 7, 2001; In Final Form: September 27, 2001

A new synthesis pathway for MCM-48 is developed using fumed silica as the silicate source and a Gemini surfactant (GEM 16-12-16) as the surface directing agent. Different synthesis parameters have been optimized in order to obtain a highly ordered mesostructure. The determining factor in the stabilization of the final structure is proven to be a double post-synthesis hydrothermal treatment. This treatment, performed successively in a minimum of pure water at 403 K, reduces the pH of the gel, allowing a better condensation of the silicate structure. Other parameters of importance are the OH^-/Si ratio, the gelation time, and the synthesis temperature, influencing the solubility of the fumed silica, the condensation and the structuring of the silicate framework, and the pore diameter, respectively. The synthesis temperature has also a positive effect on the particle dimension, producing uniform grains of 4−5 μm. The optimized parameters (3-day gelation time followed by two consecutive post-synthesis hydrothermal treatments) give a highly reproducible synthesis, with a high silica yield (70−75%). The synthesized samples have been characterized using XRD, N_2 sorption isotherms, SEM, and infrared (DRIFT) measurements.

Introduction

Since the development of the first mesoporous materials in the early nineties, one of the main objectives has been a further rationalization of the synthesis procedure, thus maximizing reproducibility and yield without reducing the ordering of the samples. MCM-48, the cubic phase of the M41S mesoporous family, received very little attention in the optimization due to its challenging synthesis and the difficulties in structure characterization. This has left the potential applications fairly undiscovered. The unique, well-ordered, three-dimensional pore structure makes those mesostructures very interesting for catalysis and chromatography.[1,2]

However, already a few important steps have been taken in optimizing the synthesis of MCM-48.[3] One of the most groundbreaking innovations has been the introduction of the Gemini surfactant by Huo et al.[4] These surfactants influence the *g* packing parameter giving preferentially the cubic MCM-48 phase. Their general formula: $[C_nH_{2n+1}N^+(CH_3)_2-(CH_2)_s-N^+(CH_3)_2C_mH_{2m+1}].2Br^-$ is denoted as GEM *n-s-m*. Huo et al. also introduced a post-synthesis hydrothermal treatment improving greatly the long-range ordering. His procedure consisted in collecting the synthesized MCM-48 gel by filtration and resuspending the solid in pure water for a hydrothermal treatment during an additional amount of time. Van Der Voort et al.[5] further optimized the MCM-48 synthesis, using different Gemini surfactants, and significantly decreased the synthesis time without loss of the quality of the materials. A post-synthesis hydrothermal treatment at 373 K proved to give the best results.

Other authors[6,7] used the post-synthesis hydrothermal treatment in the MCM-41 synthesis mainly to increase the pore size. They performed their post-treatment at higher temperature (423 K) compared to the synthesis temperature. Kruk et al.[8] proposed that synthesis temperatures above 423 K induce a partial decomposition of the cetyltrimethylammonium bromide surfactant to form dimethylhexadecylamine (DMHA), which would act as a cosurfactant, enlarging the micelle volume and thus the pore width.

All the above-described synthesis procedures of MCM-48 used tetraethyl orthosilicate (TEOS) as the silica source. During its hydrolysis, large quantities of ethanol are released. Ethanol is necessary when the cetyltrimethylammonium surfactant molecule is used in the synthesis of MCM-48. It will incorporate the hydrophobic part of the surfactant rod near the polar headgroups. This creates the correct volume in the *g* packing factor in order to induce the cubic mesophase. This has been demonstrated using fumed silica as silica source.[3,9] But such mechanism remains difficult to control. However, when a Gemini surfactant is used, the *g* packing factor is already optimal to achieve a MCM-48 structure. Therefore, the use of the expenseieve and hazardous TEOS is no longer required. Moreover, the use of TEOS has shown to produce rather low synthesis yields (30%).

In this study, fumed silica has been used as silica source together with the Gemini surfactant. The influence of the different synthesis parameters is discussed. Especially, the post-synthesis hydrothermal treatment is an important factor, determining the quality of the final material.

Experimental Section

The Gemini surfactant GEM 16-12-16 (GEM *m-s-n*) is prepared by refluxing 1,12-dibromododecane (*s*) and *N*,*N*-dimethylhexadecylamine ($n = m$) respectively, in acetone for 24 h, followed by recrystallization from acetone. The MCM-

* Corresponding author. E-mail: olivier.collart@ua.ac.be.
† University of Antwerp.
‡ Ecole Nationale Supérieure de Chimie de Montpellier.

10.1021/jp013037u CCC: $20.00
Published on Web 12/05/2001

48 is synthesized by dissolving the surfactant in water together with the base (NaOH expressed as OH^-) under vigorous stirring. After half an hour the fumed silica (Aerosil 380) is added and the solution is stirred for another 30 min. The molar gel composition is $Si/OH^-/H_2O$/surfactant = 1/0.26/100/0.1. Subsequently the gel is transferred into a Teflon-lined autoclave at a chosen reaction temperature (between 373 and 423 K) for several days in order to synthesize the "mesogel". This procedure is referred to as the gelation procedure. After a well-determined gelation time, the gel is then recovered by filtration, washed with 15 mL of deionized water per gram of fumed silica, and resuspended in deionized water (15 g per gram of fumed silica) for 24 h at the same temperature as the gelation temperature. This post-synthesis hydrothermal treatment is repeated once more. The final product is then calcined in ambient air from room temperature up to 823 K with a heating rate of 2 K/min.

Other experiments were performed by pH adjustment instead of the water treatment. The pH decrease is performed by adding dropwize a 0.1 M acetic acid solution under vigorous stirring to the synthesis gel. The pH is decreased with 0.1 pH/min till 10.5 and maintained at this stage for half an hour by readjustments before continuing the pH decrease until it reaches 10. The pH is then constantly readjusted in order to keep it invariable for at least 1 h. After the pH decrease, the gel is reheated at 388 K for 24 h before being recovered.

The N_2 sorption isotherms are recorded on a Quantachrome Autosorb-1-MP automated gas adsorption system. The surface area is calculated using the well-known BET method. The total pore volume is determined just after the capillary condensation step to exclude interparticle mesoporosity in the calculations. All reported pore diameters represent the maximum of the pore size distributions (PSD). Those are calculated using the Kruk-Jaroniec-Sayari (KJS) model.[10,11] This model has been optimized for MCM-41 but gives also a very good approximation of the PSD for MCM-48.[12] To test the validity of this method, a few PSD have been calculated using the NLDFT.

X-ray diffraction patterns were collected on a Philips PW1840 powder diffractometer (45 kV, 25 mA) using a Ni-filtered Cu Kα radiation. Diffuse Reflectance Infrared Fourier Transform spectra (DRIFT spectra) were recorded on a Nicolet 20SXB FTIR spectrometer, equipped with a Spectra-Tech diffuse reflectance accessory. The resolution was 0.5 cm^{-1}, and 100 scans were taken of a 2 wt % diluted sample in KBr.

SEM images were recorded using a JEOL-JSM-6300 scanning electron microscope operating at an accelerating voltage of 20−30 kV. The samples were sputtered with a thin film of gold.

Results and Discussions

a. Post-Synthesis Hydrothermal Treatment. The procedure of the post-synthesis hydrothermal treatment consists of recovering the gel by filtration after 3 days gelation time at 388 K and resuspending it in pure water for 24 h at 403 K. This procedure is performed twice.

The N_2 sorption isotherms of the calcined samples after the different synthesis steps are presented in Figure 1. Two major trends can be observed, related to the successive post-treatment: (1) an increase of the total pore volume, and (2) a shift of the capillary condensation step to higher relative pressure. The total pore volume increases with 53% up to 0.83 cm^3/g during the first post-treatment and it is less affected (+6%) by the subsequent post-treatment. The observed shift to higher P/P_0 of the capillary condensation, associated with pore enlargement, occurs during the two post-treatments and reaches a maximum of 32 Å (Table 1).

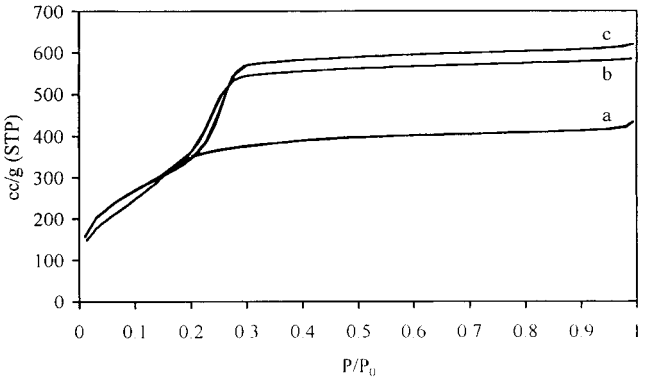

Figure 1. N_2 sorption isotherms at 77 K of a calcined MCM-48 obtained after the gelation procedure (a) and the same sample after the first (b) and second (c) post-synthesis hydrothermal treatments.

TABLE 1: The Influence of the Post-Synthesis Hydrothermal Treatments on the Physical Characteristics of a Calcined MCM-48

	treatment		
	mesogel	first post-treatment	second post-treatment
pore diameter	26 Å	30 Å	32 Å
tot. pore volume	0.54 cm^3/g	0.83 cm^3/g	0.88 cm^3/g
a before calc.	8.61 nm	8.61 nm	8.61 nm
a after calc.	7.54 nm	7.69 nm	7.98 nm
$\langle D \rangle$	10 Å	10 Å	10 Å
pH	11	10.4	9.1

The unit cell parameter a_0 is calculated out of the XR diffractograms using the formula $a_0 = d(h^2 + k^2 + l^2)^{1/2}$. Table 1 reveals that the unit cell parameter of the uncalcined samples remains unaffected by the different treatments to stay invariably at 86 Å. But, decreases of a_0 are observed after calcination pointing out a contraction of the unit cell. This contraction is high (15% or 1.28 nm) for the samples which have not been post-treated. The post-synthesis hydrothermal treatment thus stabilizes the structure and reduces the contraction. The second post-treatment is the most effective. The unit cell reduces with 11% (0.92 nm) after the first post-treatment and only 7% (0.63 nm) after the second post-treatment. A value of 0.5 nm contraction is often observed on the MCM-41 synthesis.[13]

The post-treatments induce a pH decrease in the slurry (Table 1) which allow a better stabilization of the structure, resulting in larger and more uniform pores after calcination.

The pore wall thickness $\langle D \rangle$ has been calculated from the pore diameter (d_p) and the unit cell parameter a_0, according to the formula described by Ravikovitch et al.:[14,15] $\langle D \rangle = (a_0/3.092) - (d_p/2)$, 3.092 being a constant representing the minimal surface area for the MCM-48 *Ia*3*d* space group. The calculated pore wall thickness is reported in Table 1. The pore wall thickness is not influenced by the hydrothermal post-treatment, showing that the pore expansion is solely due to the significant reduction of the unit cell contraction during the calcination process.

Less contraction implies a better stabilized structure. The reasons for this can be sought in the evolution of the pH during the different treatments. In Table 1, a pH decrease from 13 to 11 is reported for the basic mother solution after 3-day synthesis. The post-treatments further decrease the pH of the gel to 10.4 for the first post-treatment and 9 for the second. For the subsequent hydrothermal post-treatments the pH stabilizes at 9. When those pH data are superposed on the dissolution curve

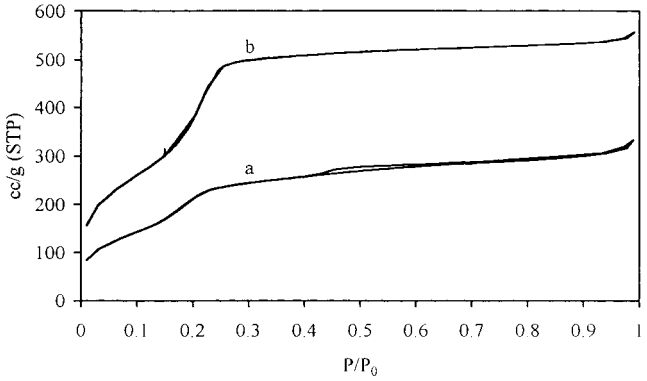

Figure 2. N_2 sorption isotherms at 77 K of a calcined MCM-48 obtained after the gelation procedure (a) and the same sample after the first post-synthesis treatment (b).

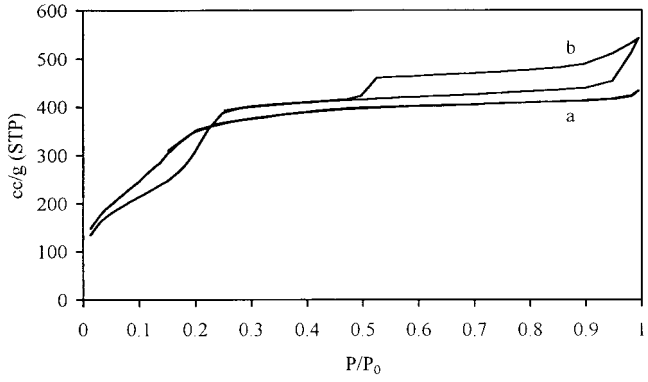

Figure 3. N_2 sorption isotherms at 77 K of a calcined MCM-48 obtained after the gelation procedure without (a) and with (b) a pH correction to 10 with 0.1 M acetic acid.

of fumed silica,[16,17] one can observe that a pH decrease favors the silicate condensation. A better condensed structure suffers less contraction during the calcination due to the presence of a higher number of more stable siloxane bridges. The highest condensation occurs pricipally during the second post-treatment due to the largest pH decrease. This confirms the aforementioned conclusions of the N_2 sorption isotherm where the second post-treatment was found to be the structure stabilizing step.

During the first post-treatment the pH drops slowly from 11 to only 10.4. This high pH still allows silica to dissolve. Therefore a silica dissolving−condensation equilibrium is recreated in the pure distilled water. This permits the structure to reorganize into a better MCM-48 structure by redissolving part of the structure. This is demonstrated in Figure 2. The hysteresis clearly visible after 3 days of gelation in the basic mother solution (Figure 2a) completely disappeared after the first hydrothermal treatment (Figure 2b).

It is therefore possible to claim that the first post-synthesis hydrothermal treatment will not only stabilize the structure by a pH decrease, but also permits reorganization of the structure. Only during the second post-synthesis hydrothermal treatment will the pH be low enough (pH 9) to have a determined effect on the condensation of the structure and therefore a double post-synthesis hydrothermal treatment is necessary.

b. pH Adjustment. To further investigate the pH effect on the stabilization of the structure during the post-synthesis hydrothermal treatments the pH is decreased with a 0.1 M acetic acid solution. Ryoo[13] already used this method in the synthesis of MCM-41, improving the long-range structural order and textural uniformity.

Figure 3 shows the isotherms of a calcined sample after synthesis in a basic medium (Figure 3a) and the same sample after pH adjustment to 10 with 0.1 M acetic acid (Figure 3b). The adjustment allows the increase of the pore size up to 30 Å. Calculations of the wall thickness give an invariable thickness of 9 Å, meaning that the increase of the pore diameter can be fully attributed to a smaller unit cell contraction during the calcination, compared to the untreated sample.

A hysteresis appears at higher relative pressure, typical for interparticle mesoporosity, as a result of particle condensation due to the pH decrease. The total pore volume increases less than in the case of post-synthesis hydrothermal treatment. This method is less adequate for the structure stabilization.

The condensation of the silicate framework is further studied by infrared (DRIFT) spectroscopy. Figure 4 shows the infrared absorption region of the silicate framework vibrations of MCM-48 before (Figure 4a,b) and after (Figure 4c,d) calcination of the untreated (a,c) and treated (b,d) gel with 0.1 M acetic acid.

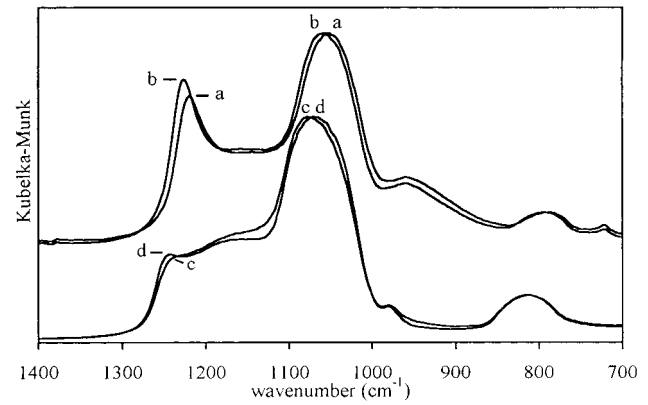

Figure 4. DRIFT spectra of the silica framework vibrations of an uncalcined MCM-48 without (a) and with (b) a pH adjustment to 10 with 0.1 M acetic acid; (c) and (d): the same samples after calcination, respectively.

The 1230−1240 cm^{-1} infrared band represents the asymmetric stretching absorption band of strained siloxane bridges.[18] The sharpness of this absorption band is associated with the presence of a particular siloxane bridge having the same bond length all over the structure. During synthesis, the specific arrangement of the organic molecules supports an ordering of the structure at the surface−silicate interface. A well-condensed structure will preserve those types of bonding during the calcination process. The 1240 cm^{-1} infrared band must therefore be associated with siloxane bridges at the surface of the pore walls. The large absorption between 1100 and 1050 cm^{-1} is a superposition of different silicate infrared absorption bands, of which the major contribution is the asymmetric silicate stretching vibration.[19] With the pH adjustment, the infrared absorption band of the strained siloxanes (Figure 4b) is sharper than the band of the untreated sample (Figure 4a) due to more homogeneous repartition of siloxane. Simultaneously, a shift of 8 cm^{-1} to higher wavenumber is observed for both the surface and the bulk asymmetric stretching vibration (1220 cm^{-1} to 1228 cm^{-1} and from 1055 cm^{-1} up to 1061 cm^{-1}, respectively). This is a consequence of a slight increase in the bond strength due to shortening of the silicate bonds. A more condensed silicate framework is obtained after pH adjustment. The framework stabilization is more pronounced when the spectra of the uncalcined structures are compared to the ones after calcination. During the calcination of the untreated gel the asymmetric stretching vibration band shifts upward with almost 20 cm^{-1} up to 1075 cm^{-1} (Figure 4c). On the other hand, the band of the treated gel shifts only 10 cm^{-1} upward to 1071 cm^{-1} (Figure

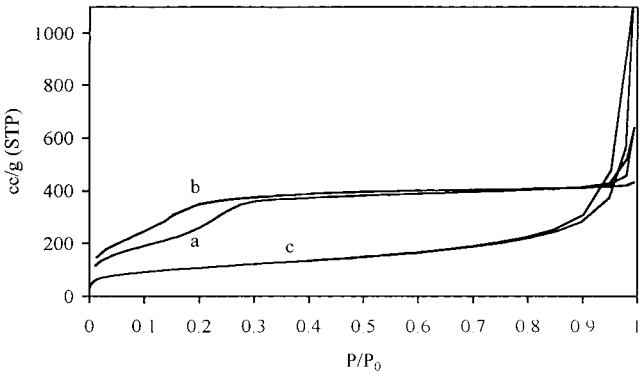

Figure 5. N_2 sorption isotherms at 77 K of a calcined MCM-48, before the post-synthesis hydrothermal treatments, synthesized with a OH^-/Si ratio of 0.20 (a) and 0.26 (b). The Aerosil 380 isotherm (c) is given for comparison.

TABLE 2: The Influence of the Alkalinity on the Physical Characteristics of a Calcined MCM-48 before Post-Synthesis Hydrothermal Treatments

	alkalinity	
	0.20	0.26
pore diameter	32 Å	26 Å
$\langle D \rangle$	8.5 Å	9 Å
pH	10.4	11

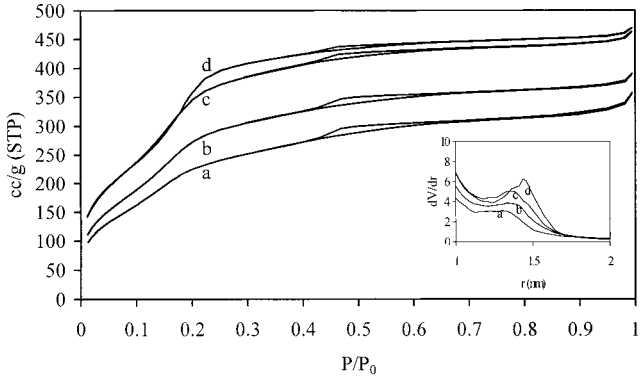

Figure 6. N_2 sorption isotherms at 77 K of a calcined MCM-48 obtained after 24 h (a), 48 h (b), 72 h (c), and 96 h (d) gelation time. Inset: the pore size distribution of the same samples.

TABLE 3: The Influence of the Gelation Time on the Physical Characteristics of a Calcined MCM-48 before Post-Synthesis Hydrothermal Treatments

	treatment			
	24 h	48 h	72 h	96 h
pore diameter	26 Å	26 Å	26 Å	28 Å
tot. pore volume	0.37 cm^3/g	0.45 cm^3/g	0.57 cm^3/g	0.61 cm^3/g
$\langle D \rangle$	9 Å	9 Å	9 Å	9 Å
pH	11	11	11	11

4d). The average siloxane bonds in the treated gel are thus less subject to contraction than those of the untreated gel.

Therefore, a precondensation by decrease of the pH prevents an uncontrolled condensation during the calcination. But the pH decrease has to occur slowly in order to permit further restructuring of the cubic MCM-48.

c. Effect of the Alkalinity. The above described results already indicated the importance of the pH in the synthesis procedure. Another important parameter to study is therefore the alkalinity in the synthesis gel determined by the OH^- (NaOH) concentration in the basic mother solution. Di Renzo et al.[20] showed that a reduction of the OH^-/Si ratio in the MCM-41 synthesis increased the wall thickness, which also improves the stability of the sample.[21] In the following experiment the OH^-/Si ratio has been reduced from 0.26 to 0.20 (expressed as the 0.26 sample and 0.20 sample, respectively).

Figure 5 represents the N_2 sorption isotherms of the calcined 0.20 (Figure 5a) and 0.26 (Figure 5b) samples after the gelation time without post-synthesis procedure). The effect of the OH^-/Si decrease is clearly observable with the capillary condensation step at a higher P/P_0 for the 0.20 sample compared to the 0.26 sample. This indicates larger pores (32 Å, see Table 2) for the 0.20 sample compared to the 0.26 sample (27 Å). The pH measurements of the mesogel reveal that a lower OH^- concentration in the mother solution indeed induces a greater reduction of the pH during the gelation step. The final pH of the basic mother solution for the 0.2 sample is 10.4 whereas its pH is 11 for the 0.26 sample. Calculations of the wall thickness indicate that the OH^- decrease has no influence on the wall thickness after calcination, contrary to the MCM-41 studied by Di Renzo.

The N_2 sorption isotherm of the 0.20 sample shows a hysteresis at high relative pressure (>0.95 P/P_0) where it is absent in the 0.26 sample isotherm. This hysteresis is comparable to the one found in the isotherm of fumed silica (Figure 5c), suggesting that part of the fumed silica used as silica source has not been dissolved. A minimum OH^-/Si ratio of 0.26 is therefore necessary to guarantee a good dissolution of the fumed silica. This absence of influence together with the relative slow structuring of MCM-48 are indications of a relatively complex built-up system for the cubic mesophase. The alkalinity of the solution does most probably not affect the formation of the MCM-48 structure but will mainly influence the stability by favoring the condensation with lower alkalinity.

d. Gelation Time. Van Der Voort[5] demonstrated, using TEOS as silicate source, that a 5-day gelation time was necessary in order to increase the long-range ordering of the MCM-48. However, 24 h are enough to prepare high quality MCM-41 using fumed silica as silica source.[22] This points out the necessity of a study on the gelation time in order to determine the optimal time required to produce high quality materials.

Figure 6 depicts the evolution of the isotherm of the gel before any post-synthesis hydrothermal treatment as a function of the time. Table 3 reports the numerical data. During the first 72 h (Figure 6a−c) an important increase in the total pore volume occurs without any enlargement of the pores (Table 3). After 72 h, the total pore volume stabilizes and the steepness of the capillary condensation step increases, suggesting a constriction of the pore size distribution (inset Figure 6). Increasing the synthesis time with another 24 h only enhances the stability of the mesogel and can thus be easily replaced by the post-synthesis hydrothermal treatment. Therefore a 72-h gelation time is sufficient. Knowing that the pH of the gel stays invariably at 11 (Table 3) during the gelation process, an equilibrium has to exist between condensation and dissolution of the structure. This equilibrium favors the formation of a well-structured MCM-48 by eventual restructurations.

The enhancement in ordering with longer gelation time can be followed in the infrared absorption region of the silica framework after calcination (Figure 7). The infrared spectra before calcination (not shown) gives a small increase of the 1240 cm^{-1} absorption band with increasing gelation time which is attributed to an increasing number of siloxane bridges. The sample with the longest gelation time has also the smallest loss of the infrared absorption intensity for the surface asymmetric stretching vibration band (around 1240 cm^{-1}) (Figure 7 inset).

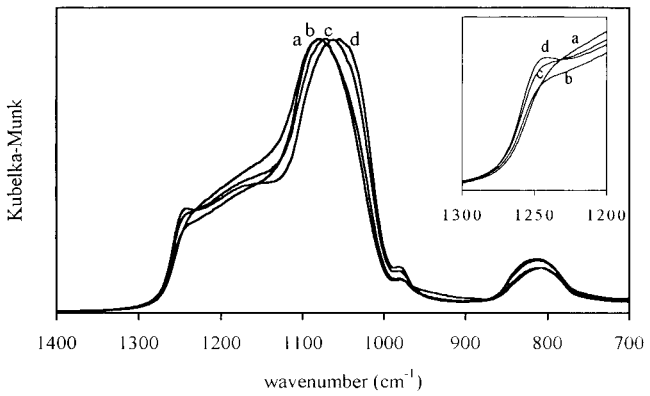

Figure 7. DRIFT spectra the silica framework vibrations of a calcined MCM-48 obtained after 24 h (a), 48 h (b), 72 h (c), and 96 h (d) gelation time.

At the same time the large band around 1060 cm^{-1} shifts to a higher wavenumber with the smallest shift for the longest gelation time. This shift corresponds to an increase of the amorphous character of the structure. Those observations indicate that the structure withstanding the best the calcination procedure is the one with the best condensed and organized silicate framework. And this can be achieved only by extending the gelation time up to 3 days minimum.

The above given results demonstrate thus that in order to obtain a good structured MCM-48 which will better withstand the calcination procedure, a gelation time of at least 3 days is necessary.

e. Temperature. All previously published articles[3−5,15,23] about MCM-48 presented structures with smaller mesopores (around 30 Å) compared to the MCM-41 (40 Å), although the surfactant chain lengths were equivalent (C_{16}). Several publications demonstrated the possibilities of pore size expansion of an MCM-41 by a temperature increase during the synthesis. In most cases the temperature exceeded 423 K, which allowed Kruk et al.[8] to conclude that the expansion mechanism is based upon decomposed surfactant endorsing the role of cosurfactant. No comparable studies have been performed on MCM-48.

Figure 8 A presents the isotherms of the MCM-48 synthesized at different temperatures (373, 388, 403, and 423 K) during 3 days followed by a post-synthesis treatment in water at the same temperature. The pore diameter increases unambiguously with a temperature increase up to 403 K (inset Figure 8A). At this temperature a maximum of 38 Å pore diameter is reached. Higher synthesis temperatures (423 K) do not further induce pore enlargement. This fact together with the observation that 403 K is beyond the decomposition temperature of the surfactant, excludes any pore increase mechanism due to a cosurfactant effect. Table 4 indicates that a higher synthesis temperature enlarges also the unit cell before calcination. Those dimensions, measured on dry samples, are identical to the ones from the same sample measured just after warm filtering. This means that the unit cells are dimensioned during the synthesis. A possible mechanism for the unit cell increase could therefore be a thermal expansion of the surfactant micelles. The maximal expansion at 403 K giving a pore diameter after calcination of 38 Å is very close to the maximal diameter of 41 Å achievable for the MCM-41 which could be expected for surfactants with the same chain length (C_{16}).

An increased synthesis temperature has also a positive effect on the structure. Figure 8B shows the N_2 sorption isotherm of samples prepared at 373 K (a), 403 K (b), and 423 K (c) before post-synthesis hydrothermal treatment. A small hysteresis at

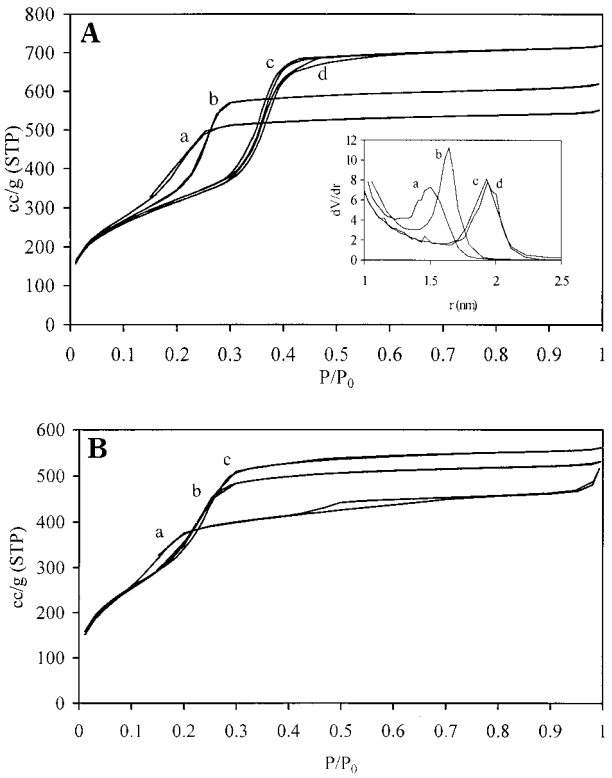

Figure 8. (A) N_2 sorption isotherms at 77 K of a calcined MCM-48 obtained after 3 days gelation time and 2 post-synthesis hydrothermal treatments at 373 K (a), 388 K (b), 403 K (c), and 423 K (d). (B) N_2 sorption isotherms at 77 K of a calcined MCM-48 obtained after 3-day gelation time at 373 K (a), 403 K (c), and 423 K (d).

TABLE 4: The Influence of the Temperature on the Unit Cell Dimension of a Uncalcined MCM-48 after Post-Synthesis Hydrothermal Treatments

	temperature			
	373 K	388 K	403 K	423 K
a_0 before calc.	83.1 Å	86.1 Å	96.1 Å	98.2 Å

$P/P_0 > 0.9$ is observed in the isotherm of the 373 K sample comparable to the one found in the isotherm of fumed silica (Figure 5c) probably coming from an uncompleted dissolution of fumed silica. The presence of amorphous silica disturbs also the ordering of the cubic mesophase as demonstrated with the hysteresis at P/P_0 0.5 associated with interparticle mesoporosity. Only at higher temperature ($T > 373$ K) could a complete dissolution of the fumed silica be obtained in order to form a well-structured mesophase. This is reflected in the XR diffractogram of the calcined sample synthesized at 403 K (Figure 9) where the absence of a broad diffraction between 20 and 25° 2θ excludes the presence of an amorphous phase.

A better ordering of the mesophase at higher temperature is also observable in the infrared spectrum of the calcined structure synthesized at 403 K (Figure 10). The silicate framework vibration region shows sharp and well-defined infrared absorption bands reflecting the presence of a well-ordered almost crystalline structure.

Furthermore, the synthesis temperature also determines the particle size of MCM-48. This is measured using a SEM image of MCM-48 synthesized at 373 K (Figure 11A) and 403 K (Figure 11B). At lower temperature, a lot of small particles (size in the range of 0.5−1 μm) are detected besides larger particles (4 μm). At higher synthesis temperature, the average particle diameter increases up to 4−5 μm with almost no small particles. This is the result of an Ostwald ripening process[16] during the

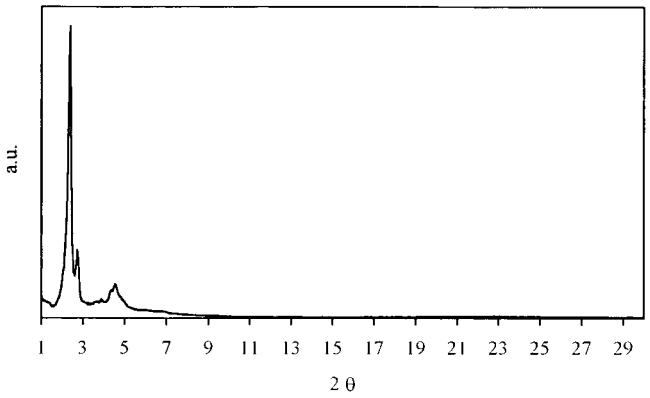

Figure 9. XRD of a calcined MCM-48 obtained after 3-day gelation time and 2 post-synthesis hydrothermal treaments at 403 K.

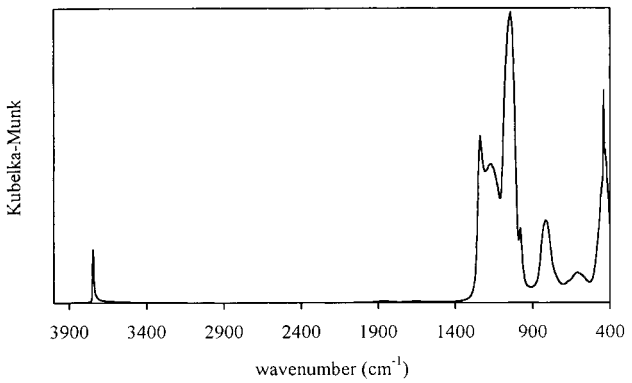

Figure 10. DRIFT spectrum of a calcined MCM-48 obtained after 3-day gelation time and 2 post-synthesis hydrothermal treaments at 403 K.

extended gelation time. This process involves a simultaneous process of dissolution and recondensation of the dissolved silica onto the surface of the remaining particles. This results in the disappearance of the smaller particles. The deposition of the dissolved silica on the remaining larger particles permits then an increase in their average size. This process stops when the difference in solubility between the smallest versus the largest particles becomes negligible resulting in a final average particle size depending on the synthesis temperature.

The particles synthesized starting from fumed silica are also 5 to 10 times larger than the ones obtained with TEOS as silica source (0.5−1 μm) (Figure 11 C).

f. Reproducibility and Yield. The constant equilibrium between dissolution and controlled recondensation of the structure during the whole formation process enables the possibility of making very reproducible materials. Five batches of MCM-48 have been synthesized using the optimized synthesis parameters. Those are a 3-day gelation period in the basic mother ($OH^-/Si = 0.26$) solution at 403 K followed by two successive double post-synthesis hydrothermal treatments in a minimum of pure water at 403 K. The characterization of the samples results in specific surface areas of 1250 $m^2/g \pm 20$, total pore volumes 1.07 $cm^3/g \pm 0.04$, and pore diameters 40 Å $\pm$ 1.

Next to the great reproducibility, high silica yields are obtained. About 70% of the silicate source is consumed in the formation of the MCM-48 structure. The other 30% are lost as dissolved silica. The yield therefore has improved with more than 100% compared to the yield of the synthesis based on TEOS. The latter has a maximum yield of 30%. This makes fumed silica an outstanding silicate source for MCM-48 formation.

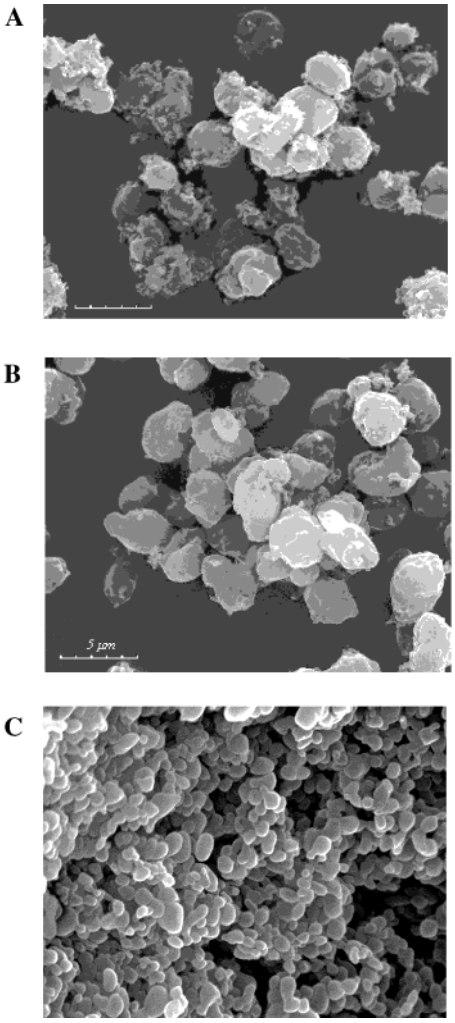

Figure 11. (A) SEM image of an MCM-48 synthesized at 373 K. (B) SEM image of an MCM-48 synthesized at 403 K. (C) SEM image of an MCM-48 synthesized from TEOS.

Conclusions

A new synthesis pathway for MCM-48 has been developed using fumed silica as a silica source. Different parameters have been studied and optimized:

1. Double post-synthesis hydrothermal treatment: The necessity of this treatment has been demonstrated. During both post-synthesis hydrothermal treatments, the pH slowly decreases, enhancing a better condensation of the silica framework. The first post-treatment causes a pH decrease to 10.4. This still allows the silica to partially redissolve, permitting the structure to reorganize into a better MCM-48. Only during the second post-treatment does the pH decrease enough (pH 9) in order to favor an optimal condensation.

2. A pH adjustment: A fast pH decrease using 0.1 M acetic acid stabilizes the structure but does not improve the structure ordering and is therefore not an alternative for a double post-treatment.

3. OH^-/ Si: A OH^-/Si ratio of 0.26 is the minimum required to dissolve completely the fumed silica source.

4. Gelation time: A prolonged gelation time improves the condensation of the structure. After 72 h, a maximum is achieved in the formation of the mesostructure. A longer gelation time leads to lower improvements.

5. Temperature: An increase of the temperature enlarges the pore diameter. This pore swelling proceeds up to 403 K and

remains at 40 Å for higher temperatures. A higher reaction temperature also favors the dissolution of fumed silica allowing a better formation of the MCM-48 structure. Finally, at higher temperatures, the average particle size of MCM-48 increases (4−5 μm) as a consequence of an Ostwald ripening process.

6. Yield and reproducibility: The synthesis of MCM-48 using the optimized parameters is highly reproducible and has a silicate yield of 70%, which is far above the 30% observed when TEOS is used as silicate source. 30% of the fumed silica is lost as dissolved silica.

The optimized synthesis parameters using fumed silica as silicate source can be summarized as follows: a 3-day gelation time at 403 K of a mesogel having a OH^-/Si ratio of 0.26, followed by two successive hydrothermal treatments of 24 h each, in pure water at 403 K.

Acknowledgment. O.C. is indebted to the IWT-Belgium for the PhD grant. P.V.D.V. acknowledges the FWO-Flanders Belgium for a postdoctoral fellowship. The authors acknowledge Mr. Schrijnemakers for performing the XRD-measurements and Mr. Dorrine for recording the SEM images.

References and Notes

(1) Corma, A. *Chem. Rev.* **1997**, *97*, 2373.
(2) Raimondo, M.; Perez, G.; Sinibaldi, M.; De Stefanis, A.; Tomlinson, A. A. G. *J. Chem. Soc., Chem. Commun.* **1997**, 1343.
(3) Morey, M. S.; Davidson, A.; Stucky, G. D. *J. Porous Mater.* **1998**, *5*, 195.
(4) Huo, Q.; Margolese, D. I.; Stucky, G. D. *Chem. Mater.* **1996**, *8*, 1147.
(5) Van Der Voort, P.; Mathieu, M.; Mees, F.; Vansant, E. F. *J. Phys. Chem. B* **1998**, *102*, 8847.
(6) Corma, A.; Kan, Q. B.; Navarro, M. T.; PerezPariente, J.; Rey, F. *Chem. Mater.* **1997**, *9*, 2123.
(7) Cheng, C.-F.; Zhou, W.; Park, D. H.; Klinowski, J.; Hargreaves, M.; Gladden, L. F. *J. Chem Soc., Faraday Trans.* **1997**, *93*, 359.
(8) Kruk, M.; Jaroniec, M.; Sayari, A. *J. Phys. Chem. B* **1999**, *103*, 4590.
(9) Gallis, K. W.; Landry, C. C. *Chem. Mater.* **1997**, *9*, 2035.
(10) Kruk, M.; Jaroniec, M.; Sayari, A. *Langmuir* **1997**, *13*, 6267.
(11) Jaroniec, M.; Kruk, M.; Sayari, A. *Stud. Surf. Sci. Catal.* **2000**, *129*, 587.
(12) Benjelloun, A.; Van Der Voort, P.; Cool, P.; Collart, O.; Vansant, E. F. *Phys. Chem. Chem. Phys.* **2001**, *3*, 127.
(13) Ryoo, R.; Kim, Ji Man. *J. Chem. Soc., Chem. Commun.* **1995**, 711.
(14) Ravikovitch, P. I.; Neimark, A. V. *Langmuir* **2000**, *16*, 2419.
(15) Schumacher, K.; Ravikovitch, P. I.; Du Chesne, A.; Neimark, A. V.; Unger, K. K. *Langmuir* **2000**, *16*, 4648.
(16) Iler, R. K. *The Chemistry of Silica*; Wiley-Interscience Publications: New York, 1979.
(17) Private communication with Degussa-Hüls.
(18) White, R. L.; Nair, A. *Appl. Spectrosc.* **1990**, *44*, 69.
(19) Holmes, S. M.; Zholobenko, V. L.; Thursfield, A.; Plaisted, R. J.; Cundy, C. S.; Dwyer, J. *J. Chem. Soc., Faraday Trans.* **1998**, *94*, 2025.
(20) Di Renzo, F.; Testa, F.; Chen, J. D.; Cambon, H.; Galarneau, A.; Plee, D.; Fajula, F. *Microporous Mesoporous Mater.* **1999**, *28*, 437.
(21) Di Renzo, F.; Desplantier, D.; Galarneau, A.; Fajula, F. *Catal. Today* **2001**, *66*, 75.
(22) Galarneau, A.; Desplantier, D.; Dutartre, R.; Di Renzo, F. *Microporous Mesoporous Mater.* **1999**, *27*, 297.
(23) Romero, A. A.; Alba, M. D.; Zhuo, W.; Klinowski, J. *J. Phys Chem. B* **1997**, *101*, 5294.